Sensors & Transducers, Vol. 201, Issue 6, June 2016, pp. 89-100

Sensors & Transducers

http://www.sensorsportal.com

An Active Plasmonic to Explore on-Chip Sensing Applications

Nan-Fu Chiu and Yu-Chieh Yen

Laboratory of Nano-photonics and Biosensors,
Institute of Electron-optical Science and Technology, National Taiwan Normal University,
No. 88, Sec. 4, Ting-Chou Road, Wenshan Dist., Taipei 11677, Taiwan
Tel.: +886-2-77346722, fax: +886-86631954
E-mail: nfchiu@ntnu.edu.tw

Received: 2 May 2016 /Accepted: 7 June 2016 /Published: 30 June 2016

Abstract: We report the influence of top emission and transparent organic electroluminescence (OEL) devices on the color tunability, viewing angle and enhancement light efficiency by surface plasmon grating coupled emission (SPGCE), the effects of coupled active SPPs on the metal nano-grating with organic material interface by cross-coupled into far-field space. Owing to the narrow band emission from the SPGCE, one can observe clear color changes at a certain viewing angle with different permittivities. The experimental and theoretical results showed that OEL-SPGCE at different pitch can match a linear shifting of momentum (ΔK) of about 4.8 μm^{-1} per 100 nm pitch size. The color changes from -1.1 degree (water), -.07 degree (glucose 10 %), -2.5 degree (glucose 20 %), to 6 degree (glucose 40 %) with the increasing permittivities. The OEL-SPGCE biosensor is proposed for the development of novel devices, which is expected to improve the capability of electroluminescent bio-plasmonic resonance measurement devices in the future. *Copyright © 2016 IFSA Publishing, S. L.*

Keywords: Surface plasmon grating coupled emission, Active plasmonic biosensors, Organic electroluminescent, Surface plasmonic resonance, Nano-grating.

1. Introduction

Surface plasmon oscillation is the collective longitudinal fluctuation of free electrons on a metallic/dielectric boundary [1]. The resonance is a result of energy and momentum being transformed from incident light into surface plasmons, and is sensitive to the refractive index of the medium in contact with the metal film. The phenomenon of anomalous diffraction on diffraction gratings or roughness due to the excitation of surface plasmon waves was initially described in the beginning of 1902 by Wood [2, 3]. A phenomenon later attributed to the excitation of surface waves and a classical theoretical analysis was given later by U. Fano [4]. In 1958 Thurbadar observed a large drop in reflectivity when illuminating thin metal films on a substrate [5], but did not link this effect to surface plasmons. Ritchie postulated the existence of surface plasmons in thin metal films penetrated by electrons at that time [6]. Their existence had then been demonstrated in electron energy-loss experiments by Powell and Swan [7, 8]. In 1967 Teng and Stern [9] have been able to construct a dispersion curve for the surface plasmon in aluminum by observing dips in the spectrum of light specular reflected from an aluminum-coated grating by Stewart and Gallawat [10] and from peak in the light emitted from the same grating bombarded by fast electrons. These anomalies, which are most important for light polarized with its electric vector perpendicular to the grating rulings, have been studied both experimentally and theoretically [11, 12]. In 1968

Otto explained Turbadar's results and demonstrated that the drop in the reflectivity in the attenuated total reflection (ATR) method is due to the excitation of surface plasmons [13].

In the same year, Kretschmann and Raether reported excitation of surface plasmons in another configuration of the ATR method [14, 15] and introduced different optical methods of surface plasmon excitation by utilizing ATR in a prism. The ATR method is very convenient and since its contrivance the field has prospered and many properties of surface plasmons (SPs) have been studied [16, 17]. Recently (1998), the phenomenon of extraordinary transmission discovered by Ebbesen et al. [18, 19] showed that EM wave transmission through a silver film with a periodic array of sub-wavelength holes [20] can be significantly higher than the conventional predictions, due to the excitation of surface plasmons. Other research fields include surface-enhanced Raman spectroscopy [21, 22] and observations of single-molecule surface-enhanced Raman scattering [23, 24], efficient dipole sources such as molecules [25, 26] or laser diodes [27, 28], infrared detectors [29, 30], distributed-feedback quantum-cascade lasers in the near-infrared [31, 32] and far-infrared [33, 34], and the enhanced transmission of fluorescence through continuous metal films [35, 36] also involve SPPs, mediate excitation energy transfer between molecules on opposite side of a metallic film [37], controlling the optical interaction between molecules in areas as diverse as photosynthesis [38] and solid-state polymer lasers [39]. In those systems, the metallic grating is exploited either for the field enhancement around the grooves or for the ability of the grating to convert evanescent waves into radiation. In 1980, Nylander and Liedberg et al. [40, 41] have demonstrated that SPR in the Kretschmann-configuration was well suited for both gas and biomolecular sensing purposes. In 1990, a commercial product came into the market: Pharmacia Biosensor introduced the BIAcore (Sweden) (BIAcore for GE Healthcare, USA) [42, 43] biosensor based on surface plasmon resonance. Development of smart sensor with high sensitivity was very popular in 21st century. Over the past ten years, SPR technology has advanced from basic refractive index measurements to much more complex applications such as bio-sensing applications, reduction oxidation, and protein-protein interaction. Their success can be attributed to their ability to detect biomolecular interactions in real time without the need for any labeling.

The motivation of this research is to develop an accurate, integrated SPR sensor system chip using existing organic light-emitting or organic electroluminescent plasmonic technology due to its sensitivity and label-free advantage.

We will propose a novel design of SPR device without using external light source and polarizer to have the same features of SPR, i.e., high sensitivity and real time. It is based on the electro-excitation of organic and metallic materials. It can induce SPR wave on the metallic surface when proper resonant condition is matched. We can then observe the signal changes due to the presence of surface molecule or specific absorption wavelength of multiple samples. We call such an active plasmonic sensor an "organic electroluminescent surface plasmon grating coupled emission sensor, (OEL-SPGCE)" [44-46]. It is an excellent system of active surface plasmon resonant biochip based on novel electroluminescent sensing method.

2. Materials and Methods

2.1. Theory for SP Grting Coupler

The first observations of surface plasmons were reported on gratings, dubbed Wood's anomalies [2]. A grating resembles a periodically corrugated surface modulation. In this method, an incoming light wave is incident from a dielectric medium (ε_d) on a metal grating with the dielectric constant (ε_m), the grating period (Λ) and the grating depth (h), as shows in Fig. 1. Use an incident light with the wave-vector k_s is made incident on the grating surface. The k_s diffraction gives rise to a series of diffracted waves [47]. The wave-vector of the diffracted light k_m is:

$$k_m = k_s + mG, \tag{1}$$

$$G = \frac{2\pi}{\Lambda} x_0 \tag{2}$$

Where m is an integer and denotes the diffraction order and G is the grating vector with the magnitude [48, 49]. If the in-plane component of the wave-vector of a give m order matches the surface plasmon dispersion relation by excited.

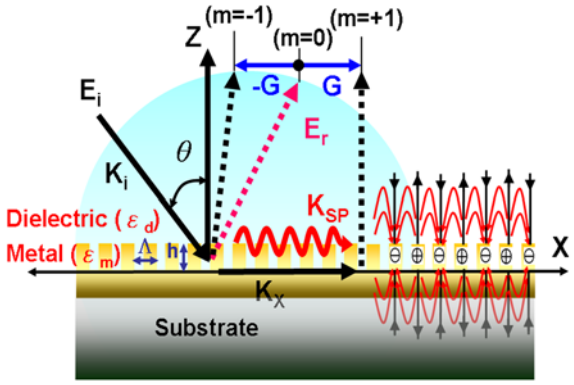

Fig. 1. Excitation of surface plasmons by the diffraction of light on a diffraction grating. A combination with a magnitude exceeding the radius results in a solution bound to the surface with an evanescent component in the direction normal to the grating.

The diffracted waves can couple with a surface plasmon when the propagation constant of the diffracted wave propagating along the grating surface k_x and that of the surface plasmon k_{sp} are equal:

$$k_x = \frac{\omega}{c}\sin\theta_i \pm mG = \frac{\omega}{c}\sqrt{\frac{\varepsilon_d \varepsilon_m}{\varepsilon_d + \varepsilon_m}} = k_{sp}$$

or more generally

$$k_x = \frac{\omega}{c}\sin\theta_i \pm \Delta k = k_{sp}, \qquad (3)$$

where Δk, is shown in Fig. 2. The vector point (P) into point (Q), stems from any perturbation in the smooth surface;
Δk =0 gives no solution of the dispersion reaction.

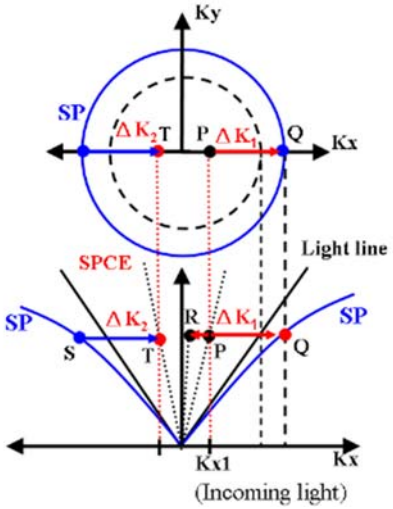

Fig. 2. The SP dispersion relation for grating coupling. SP is surface plasmon dispersion curve. The incoming light, wave-vector (K_{x1}), point (P) is transformed into a SP at point (Q), by taking up Δk_1. The interaction point (P) into point (R) via roughness leads to light scattered inside the light cone. The process point (S) into point (T) describes the decay of a SP cross-coupler into light via Δk_2.

We look at the simplest periodic plasmonic structure, the quarter wave dielectric stack. Consider light propagating normal to the interface planes. Light within a structure is no longer just an optical field, it is intimately linked with the optical response of the structure, and the mode is a polariton rather than a photon [25, 50]. The interaction between the optical field and the structure is represented by the complex dielectric permittivity and thus the complex index of refraction. As we have just seen the standing wave within the stack can have two configurations, one when the standing wave has the optical field concentrated in the high index layers, the other when it is concentrated in the low index layers. The different refractive indices of the two regions mean that the two modes have different energies. Energy band gaps can appear is equal to twice the surface plasmon modes. Two standing wave solutions are then possible Similar to the plasmonic band-gaps dispersion relation as sketched in Fig. 3. Both band-gaps in energy as well as in momentum have been reported [1, 51].

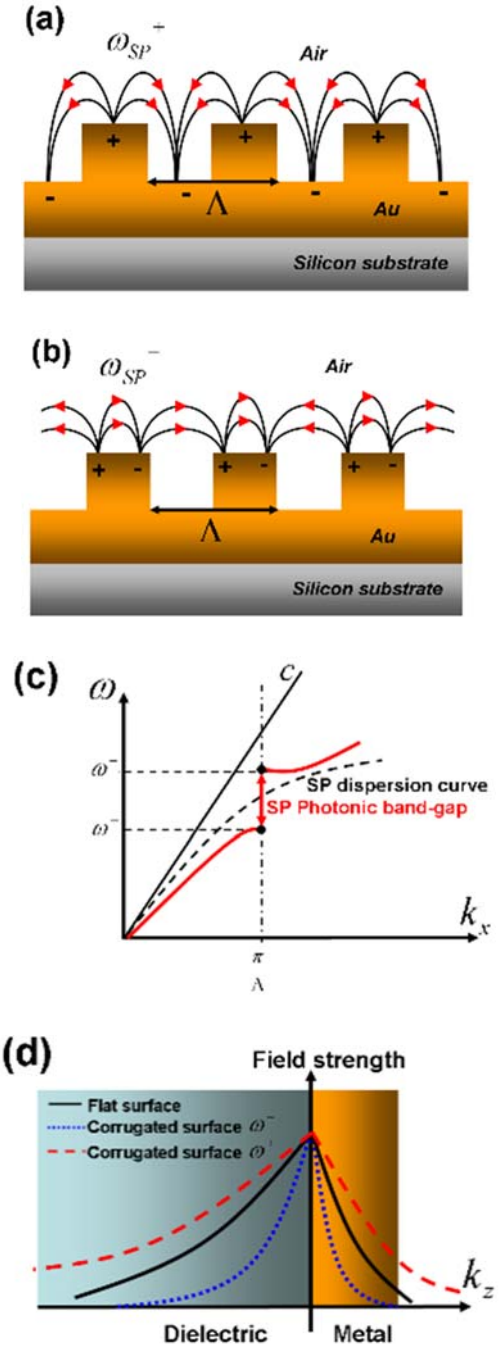

Fig. 3. Periodc structure of the metal surface can lead to the formation of an SP band-gap. SP modes with frequencies between the two band, ω^- and ω^+, and so this frequency interval is known as a stop gap. (a) and (b) The upper frequency solution ω^+ is of higher energy than ω^- because the field is more distorted. (c) The different energies related to the two standing wave solutions ω^- and ω^+ at the Brillouin zone boundary. (d) A plot of the way in which the fields decay away from the interface for the flat surface, and for the two solutions of the grating surface.

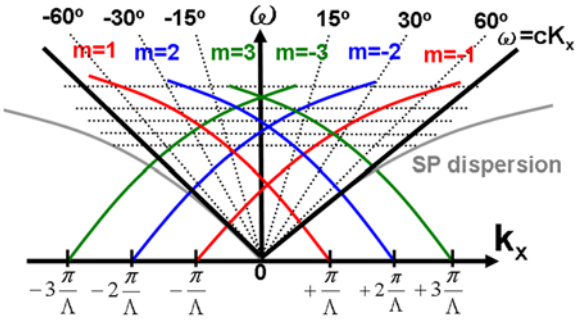

Fig. 4. The surface plasmon dispersion relation for grating coupling. The periodic grating of the surface results in dispersion relation in reciprocal space that is also periodic. In order to excite surface plasmons optically, a light source with a frequency that intersects with one of the dispersion branches is necessary.

2.2. Theory for Active Plasmon Coupler

The OEL-SPGCE transparent device is based on the fluorescent emission from the active organic EML and its diffraction in a periodically modulated surface with possible SPPs enhancement due to transparent structure of metallic thin film. Using OEL-SPGCE transparent device as a simplified model, the possible interaction mechanisms are shown in Fig. 5. When a voltage is applied between electrodes, the electrons and holes are injected from cathode and anode, respectively, into the organic layer and recombined near the junction of the EML to give light which excites the metal grating SPPs. Through radiative emission, light was generated that had optical characteristics mainly dependent on the energy levels of the active organic materials in the EML. The active organic EML serves to provide a non-oriented internal light source to generate SPPs at the metal/dielectric interface and de-coupled or cross-coupled through grating structure to give detectable radiative emission or non-radiative waveguide mode [44-46]. For OEL-SPGCE transparent device, portion of light was propagated from EML through organic layers, transparent anode and the glass substrate into the air. Since the emitted light from EML could couple with surface plasmons under matching conditions while propagating along the grating surface between the organic/metal and the metal/air interfaces, only a small portion of light from EML will be coupled out due to total internal reflection (TIR), which limits the light extraction efficiency. Therefore, there are four possible wave vectors, i.e., krad ($k_{//}$), knrad (k_w), $k_{SP(Au/air)}$, and $k_{SP(Au/Alq3)}$, that can exist between different interfaces of lamellar grating nanostructure, i.e. air, organic-layer, and two metal-dielectric interfaces. The two SP modes are associated with metal/organic and metal/air interfaces and their corresponding wave vectors are $k_{SP(Au/air)}$ and $k_{SP(Au/Alq3)}$. Such cross-coupling includes surface plasmons across the metal film and waveguide mode across the metal film. It becomes radiative emission of specific direction again through the cross-coupling of nanostructure with the emission optical properties under different diffraction orders or emission angles [52, 53].

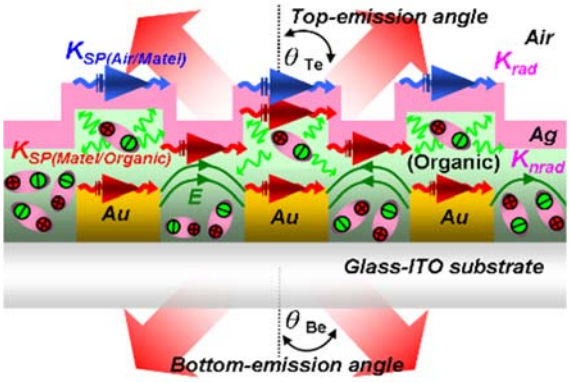

Fig. 5. Cross section view of a simplified OEL-SPGCE transparent model. The organic molecules in the EML serves to provide a non-oriented internal light source to generate SPPs at the organic/metal/dielectric interfaces and cross-couple through grating structure to give detectable radiative emission or non-radiative emission that propagates through transparent anode and the glass substrate towards the air.

The SP grating coupled emission, $k_{//}$, at certain wavelength, λ, can be resulted from the matching momentums of the internal EML emission (θ_e) through grating coupler condition (dielectric constant of EML and pitch size of Λ) to the metal/air ($Ksp_{(Ag/air)}$) and metal/air ($Ksp_{(Ag/organic)}$) dispersion curve as shown in the Eq. (4). The SP modes for Ag/air interface on the grating layer can be cross-coupled into air if its wave vector is smaller than that of the air. Eq. (5) shows the wave-vectors parallel to the surface of the emitted light. Eq. (4) and Eq. (5) give the matching condition for the guided mode of the organic layer and the de-coupling of light emission.

$$k_{SP(metal/dielectric)} = k_0 \sqrt{\frac{\varepsilon_{metal} \cdot \varepsilon_{dielectric}}{\varepsilon_{metal} + \varepsilon_{dielectric}}}, \quad and \quad k_{SP(metal/organic)} = k_0 \sqrt{\frac{\varepsilon_{metal} \cdot \varepsilon_{organic}}{\varepsilon_{metal} + \varepsilon_{organic}}} \tag{4}$$

$$k_{//} = \sqrt{\varepsilon_{organic}} \left(k_0 \sin(\theta_{emission}) \pm m \frac{2\pi}{\Lambda} \right) \tag{5}$$

3. Materials and Methods

3.1. Grating Fabrication

The samples are prepared by Electron Beam Lithography system (EBL). The EBL ELS-7500EX is scanning electronic microscope (SEM) equipped with a lithographic system [44, 47, 54]. The incident electron beam was 50 kV of the acceleration voltage.

In a first step, we used the electron-beam resist ZEP520A (To-Nippon Zeon Co.) high resolution positive electron beam resist, by spin coated about 100nm thick resist layer on silicon substrate, and pre bake temperature 180 °C for 2 minutes. After exposure of the substrate to the electron beam of the exposed ZEP520A. The shape of the individual grating was slightly elongated line patterns of grating structure with 200 nm, pitch 400 nm, exposure area 1.2×1.2 mm, pixel map 60000×60000 dots, dose timer 2 μsec. Next, a Cr film 5 nm and gold film 50 nm was by e-beam evaporated deposited onto the grating, with an evaporation rate of approximately 0.2 Å/s. Then, the remaining ZEP520A resist layer is removed by N,N Di-methylacetamide (ZDMAC, To-Nippon Zeon Co.) into a washing solution, Liftoff the gold films on ZEP520A resist. The patterning process is illustrated as shown in Fig. 6.

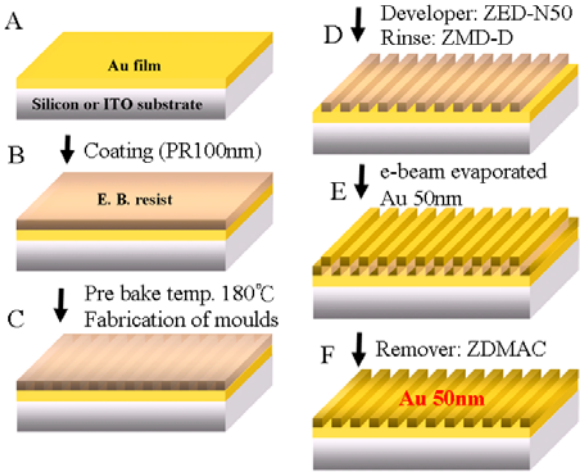

Fig. 6. Schematic flow diagram of the nanostructures patterning of metallic symmetrical lamellar grating thin films.

3.2. Active Plasmonic Device Fabrication

We prepared the nanostructure having 1-D grating pattern by electron-beam lithography (EBL) total exposure area of 1.2×1.2 mm^2. Then, the organic material was deposited on ITO and Au grating substrate by a thermal evaporator with a vacuum level and an evaporation rate of approximately $2*10^{-6}$ Torr and 0.2 Å/s, respectively. An emission area of 1.5×1.5 cm^2 was defined for the devices by sequentially depositing layers of N,N-Bis (naphthalen-1-yl) -N,N–bis (phenyl) benzidine (NPB, 80 nm), tris-(8-hydroxyquinoline) aluminum (Alq_3, 50 nm), LiF (1.2 nm) and finally Al (20 nm) as the cathode contact as to give the SP-coupled emission. After the fabrication process, the device was passivated with a 100 nm aluminum oxide (Al_2O_3) film deposited uniformly by atomic layer deposition (ALD) at temperature much lower than 90 °C within 1 hour.

3. Results and Discussion

3.1. Controlling SPR Angle of Nano-grating Structures

The patterning process is illustrated in Fig. 6. We used an EB resist mould with 1D line patterns, which was fabricated by EB lithography. Fig. 7. Shows the top-view field emission SEM (ELS-7500EX, ELIONIX CO.) images of patterned exposure gold thin films. Their surface profiles measured with atomic-force microscopy (AFM) as shown in Fig. 8. The grating profiles calculated with the unified method is shows in the figures, too. The grating heights of the AFM profiles agree well with those of the calculated profiles.

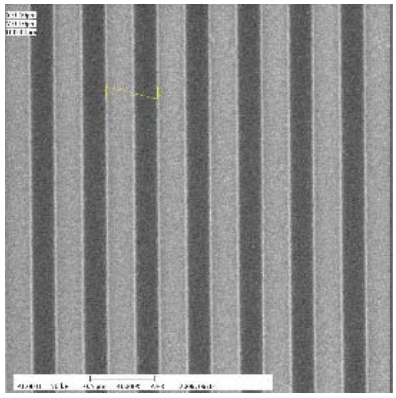

Fig. 7. The SEM of the fabricated grating and results for the line-200 nm and pitch-400 nm period grating.

The size of pitch 400 nm polymer (PR) grating-coupled SPR imaging as shown in Fig. 9. The grating-coupled SPR imaging is well suited for kinetic analysis of a wide range of biomolecular interactions of interest in the field of proteomics (antibody-antigen, protein-protein interactions, epitope mapping, etc.). This approach significantly advances conventional surface plasmon spectroscopy and allows in situ measurements of general refractive index profiles in various systems in which discrimination of spatial distribution of studied process is of interest.

Incident wave on a grating of this pitch permits momentum enhancement such that we may couple to surface plasmon resonances. These are the azimuthal-angle-dependent coupled resonance angle, where the angle and sign refer to the diffracted order that provides the resonant coupling to the SPP. The azimuthal-angle-dependent coupling SPR equation is [55]

$$k_{SPP}^2 = n_a^2 k_0^2 \sin^2\theta + \left(m\frac{2\pi}{\Lambda}\right)^2 \pm 2n_a m\frac{2\pi}{\Lambda}k_0 \sin\theta\cos\varphi \quad (6)$$

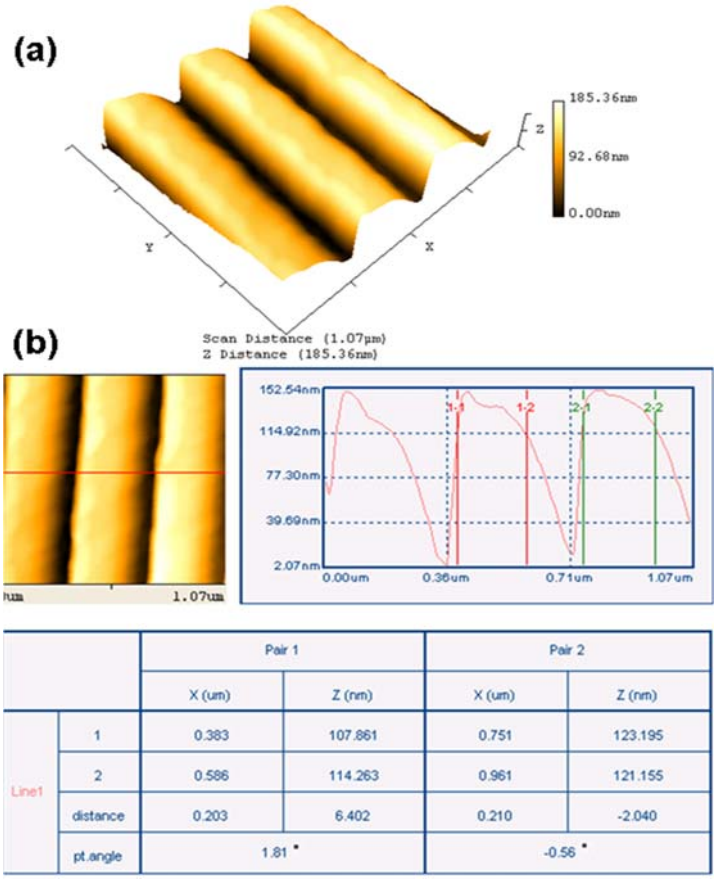

		Pair 1		Pair 2	
		X (um)	Z (nm)	X (um)	Z (nm)
Line1	1	0.383	107.861	0.751	123.195
	2	0.586	114.263	0.961	121.155
	distance	0.203	6.402	0.210	-2.040
	pt.angle	1.81 °		-0.56 °	

Fig. 8. The PR grating profiles (a) are 3D imaging and (b) used to check the shape, lateral size, and height of the structure by AFM.

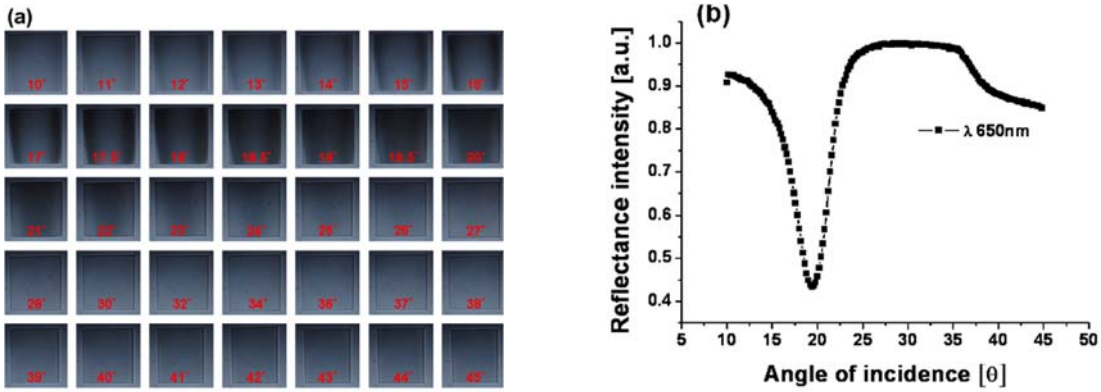

Fig. 9. (a) The grating coupled SPR imager measurements at angle of incidence, and collects the reflected light with a CCD camera. (b) Resonance angle changes on the surface are recorded as reflectance intensity.

The azimuthal angle (φ =0), by simple geometry, we find the scalar equivalent of equation (3.3) is

$$n_a \sin(\theta) \pm m\frac{\lambda}{\Lambda} = \pm\sqrt{\frac{\varepsilon_{mr} n_a^2}{\varepsilon_{mr} + n_a^2}} \qquad (7)$$

Theoretical calculation based on the Eq. (7) supports this idea as shown on the right side of Fig. 10. We calculated the SPR angle as a function of the refractive index of the Au/air layer. As the refractive index decreases, the curve shifts to the left and is accompanied by a decrease in the critical angle.

Resonance angle plots of reflectivity of a nano-grating sensor, using a different buffer layer, a pitch 400 nm and 50 nm Au grating, are shown in Fig. 11. For several refractive indices of analyte. Fig. 11 (a) and (b) demonstrates the sensitivity of a sensor with identical layers during a refractometric experiment.

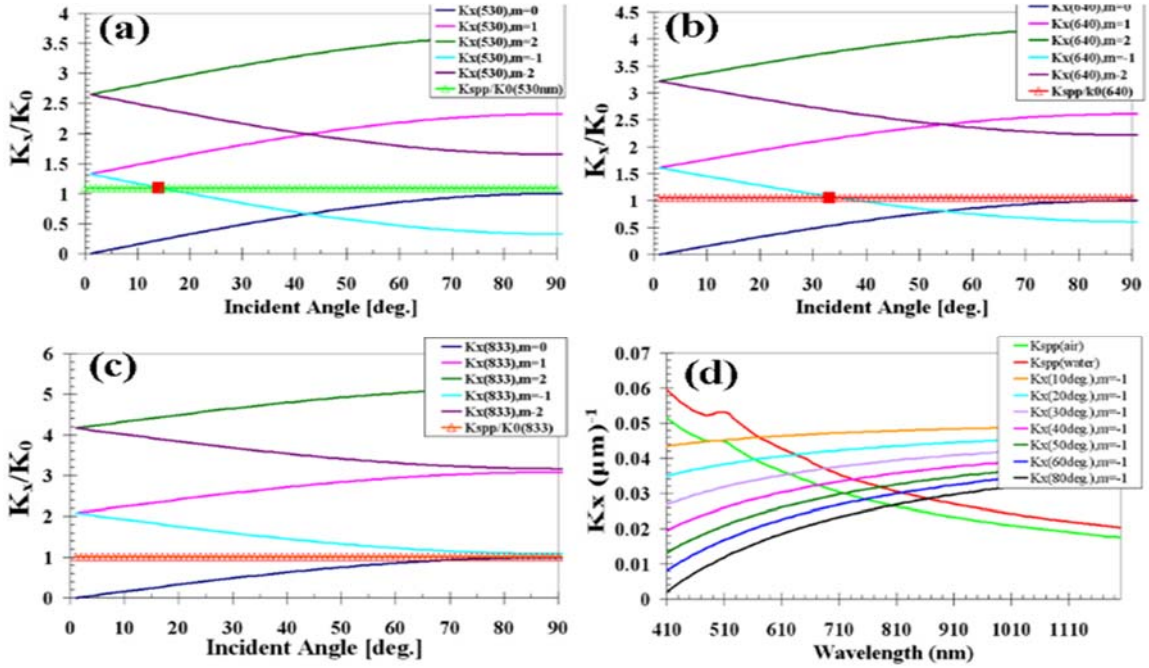

Fig. 10. Calculated SPR angle of a grating structure with pitch is 400 nm. (a) Incoming light is 530 nm, kx and Kspp dispersion match on -1st order, resonant angle 15°. (b) Incoming light is light 640nm, kx and Kspp dispersion match on -1st order, resonant angle 32°. (c) Incoming light is light 833nm, kx and Kspp dispersion no match. (d) Kspp is air and water with kx dispersion match on -1st order.

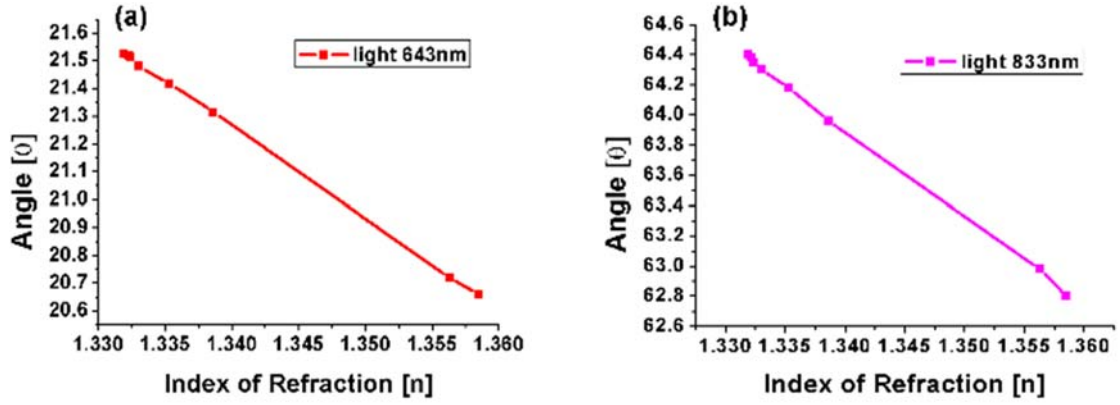

Fig. 11. Measured resonance angle for an grating sensor of a metal grating 50 nm gold and 100 nm gold film as the refractive index of the analyte was varied in steps from 1 (air) to 1.3585 (alcohol 100 %).

We considers how an energy gap for surface plasmon polaritons (SPPs) propagating on a grating can be used to modify the emission properties of an adjacent thin organic (Alq_3) layer [56, 57]. Our fabricated different pitch grating device consists of coupled organic/metal nanostructure with specific width and symmetric and asymmetric dielectric SP band gap structure. In particular it is found that emission is significantly inhibited in the vicinity of the gap, and that the modified emission spectrum is determined by the wavelength dependence of the density of SPP states. We present recent experimental results and discuss potential applications of such an active plasmonic biosensor with enhanced resonance energy emission due to interactions on the organic/metal nano-grating.

3.2. Controlling SPR Angle of Active Plasmon Structures

We report using surface plasmons excited on a metal grating to increase the emitted photoluminescence intensity from organic semiconductor film located near the Au grating. Here, we demonstrate that the luminescence enhancement is due to SP excitation. Our devices consist of organic semiconductor and metal grating. The organic semiconductor films have been thermally evaporated on top of the continuous Au grating as shown in Fig. 12.

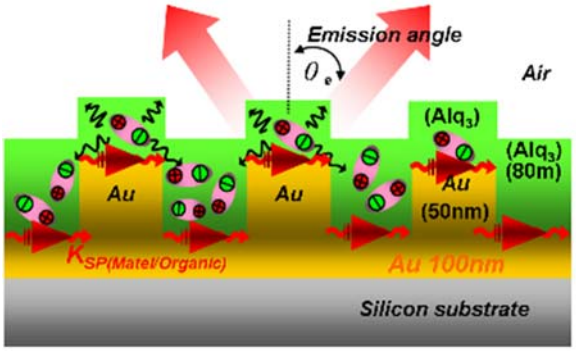

Fig. 12. Schematic diagram showing the experiment setup. The sample is a silicon based plasmonic device for the Si/Au film (100 nm)/Au grating (50 nm)/Alq3 (80 nm) structure.

Fig. 13 shows the luminescence spectra from the fabricated device as shown in Fig. 13 with (red line) and without (blue line) an Au grating. For the comparison between the two spectra to be meaningful, they have to be obtained from the same device. For the measurements shown in Fig. 13. The device has been configured for maximum surface plasmon excitation and coupled different emission angle. Remarkably, the radiation was directed into small angular distributions, in one case with over 90 % of the radiation found at two angles +30°~-30° from the normal.

This effect is not due to reflection of the emitted photons, but rather to the interactions of the oscillation dipole and the oscillations electron in the metal, and their directed radiation into the space over the metal. In the absence of a metal grating (planar metal) the emission is essentially isotropic as shown in Fig. 13 (b). This experiment arrangement is shown in Fig. 13 (c) and (d). Remarkably, the emission resulting from surface plasmon excitation is directed in a narrow angular distribution. When excitation is at the plasmon resonance angle, the emission is sharply distributed at the plasmon angle for the emission wavelength. It seems possible to use this effect to selectively observe the desired signal while rejecting background at different wavelengths or distances from the silver surface.

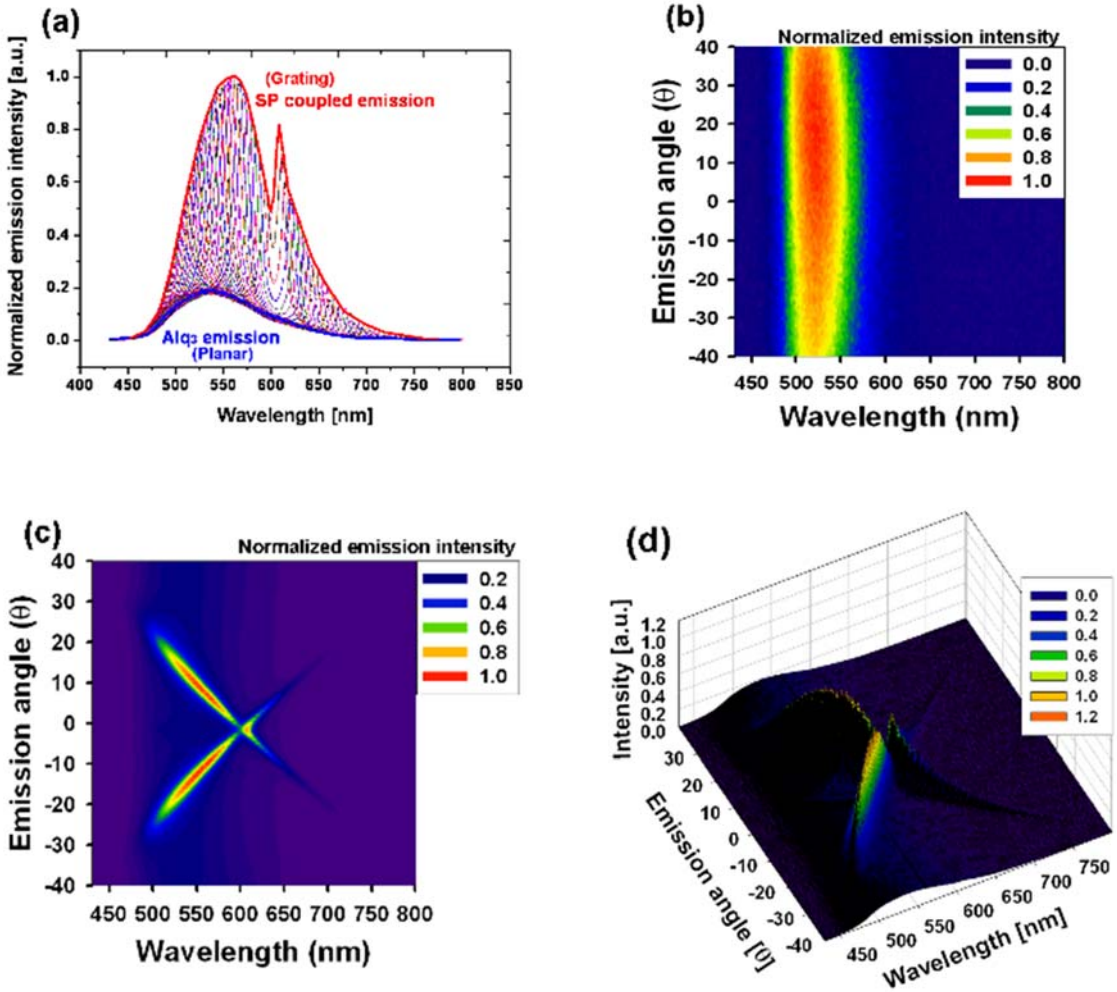

Fig. 13. Spectra of emission luminescence with and without Au grating as shown in (a). Planar metal emission is essentially isotropic as shown in (b). The device has been configured for surface plasmon excitation as shown in (c) and (d) for 3-D spectra of luminescence.

3.2. Controlling SPR Angle of OEL-Active Plasmon Structures

The OEL-SPGCE transparent device is based on the fluorescent emission from the active organic EML and its diffraction in a periodically modulated surface with possible SPPs enhancement due to transparent structure of metallic thin film. Using OEL-SPGCE transparent device as a simplified model [58], the possible interaction mechanisms are shown in Fig. 14 (a). When a voltage is applied between electrodes, the electrons and holes drift from the opposite directions, respectively, and then recombine near the junction in the emission layer (EML) to give light into excite metal grating SPPs. The SPGCE area of this green square is 1.2 mm^2. The enhancement ratio for OEL-SPGCE device on bottom emission is 3 times Fig. 14 (a). The Fig. 14 (b) is planar OLED device.

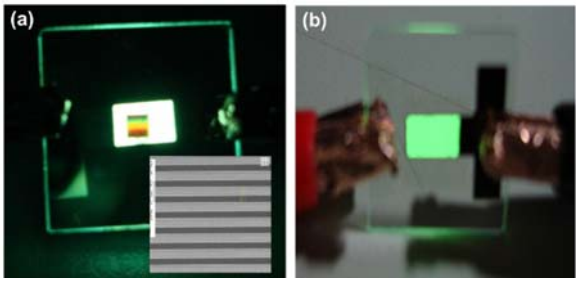

Fig. 14. Schematic diagram showing the experiment setup. The sample is a silicon based plasmonic device for the Si/Au film (100 nm)/Au grating (50 nm)/Alq3 (80 nm) structure.

The active organic EML layer can be to provide non-oriented internal light source to generate SPPs on the metal/dielectric interfaces and de-couple or cross-coupled through grating structure for detectable radiative emission or non-radiative waveguide mode. The two SP modes are associated with metal/organic and metal/air interfaces and their corresponding wave-vectors are $k_{SP(Au/air)}$ and $k_{SP(Au/Alq3)}$. Such cross-coupling includes surface plasmons across the metal film and waveguide mode across the metal film. It becomes radiative emission of specific direction again through the cross-coupling of nanostructure and the emission optical propertied under different diffraction order or emission angle [59, 60].

Fig. 15 (a, b) shows in different glucose concentration for the EL spectra at different viewing angles of the sample with pitch = 500 nm. In this measurement, spectra were taken every 0.1 degree. The emission occurred at 0º with the wavelength of 630 nm, which was 3 times higher than that of EL peak intensity of planar Alq_3 (peak at 525 nm, with full width at half maximum of 100 nm). Besides, the emission angle ranged from -0.7 to -6º covering the different concentration from glucose (1.3484) to glucose 40% (1.3968) refractive index. One can note that the color changes from -1.1 degree (water), -.07 degree (glucose 10 %), -2.5 degree (glucose 20 %), to 6 degree (glucose 40 %) with the increasing permittivities. Our device emits light with different spectra at visible range when contacting species with different relative permittivities, as shown in Table 1.

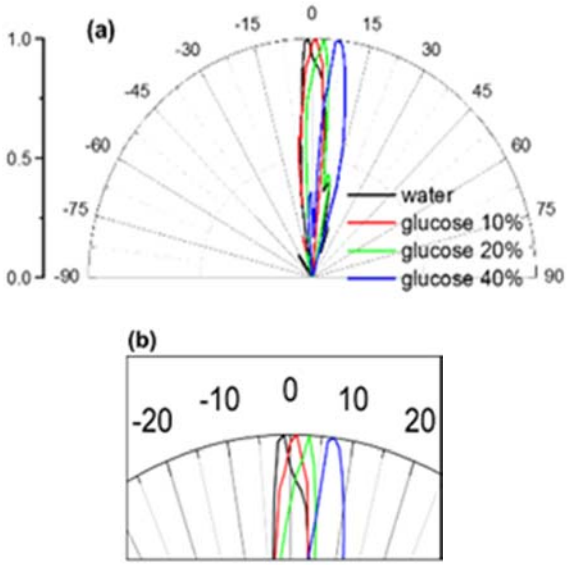

Fig. 15 (a, b). Spectral peals at different viewing angles for the OEL-SPGCE biosensors with different glucose concentration.

Table 1. Range of OEL-SPCGE emission angle (θe) and different spectra at different samples concentration.

(Pitch 500 nm)		Air	water	Glucose 10%	Glucose 20%	Glucose 40%
Angle (deg.) @ λ=550 nm	Cal.	-30	-1.1	-0.7	-2.5	6
	Meas.	-28	-2	-1	-3	7
Wavelength (nm) @ θ= 0 degree	Cal.	470.2	542.13	576.28	604.83	655.57
	Meas.	485	545	573	591	632

Fig. 16 (a) shows a dispersion relations (ω-k). solid line show the calculated (m=0) with different samples concentration. Solid symbols are the experimental data results corresponding to m=-1. Dashed lines represent calculation results of dispersion relation at Au/air interface. The experimental and theoretical results showed that OEL-SPGCE at different pitch can match a linear shifting of momentum (ΔK) of about 4.8 μm^{-1} per 100 nm pitch size. In, OEL-SPGCE biosensor experimental results, the MUA is 10 mM, DNA-1 is 0.1 mM, DNA-2 is 0.5 mM, and PL+SSMCC is 1 mM concentration. Fig. 16 (b) shows the calculation CIE coordinates results from OEL-SPGCE parameters given above, with the increasing value of refractive index for different samples concentration, one can see a right shift of the ω-k curves, which corresponds to an increase in momentum space.

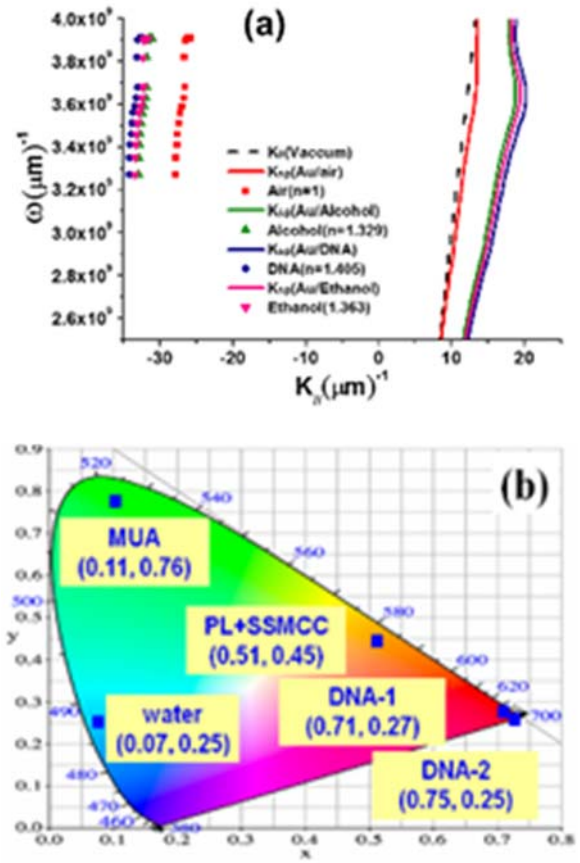

Fig. 16. (a) Calculated dispersion relation with different samples concentration, and (b) calculated CIE coordinates shift with a fixed viewing angle with different samples to be tested.

4. Conclusions

In summary, we demonstrated a highly directional active plasmonic OEL-SPCGE biosensor with different samples concentrations, which comes from the Au/sample SP radiation. Our results showed that strong SP coupling resonances in emission from the interactions of Alq3/Au and Au/sample mode leads to the enhanced directional emission, intensity and narrow spectrum. When contacting with different materials, OEL-SPCGE is sensitive to the dielectric constant. Further investigations will be performed on plasmonic with the integration of optimized active biosensors in biochemical analysis and immunoassay sensing. It is suitable for the application of low cost, point-of-care, disposable and non-labeling biosensors detection.

Acknowledgements

The authors would like to thank the Ministry of Science and Technology of the Republic of China, Taiwan, for financially supporting this research under Contract No. MOST 104-2221-E-003-023, MOST 103-2221-E-003-008, NSC 102-2221-E-003-021, and NSC 99-2218-E-003-002-MY3.

References

[1]. H. Raether, Surface Plasmons on Smooth and Rough Surfaces and on Gratings, 1, *Springer Berlin Heidelberg*, 1988.
[2]. R. W. Wood, On a Remarkable Case of Uneven Distribution of Light in a Diffraction Grating Spectrum, *Proc. of the Physical Society of London*, Vol. 18, 1902, pp. 269-275.
[3]. R. W. Wood, On a remarkable case of uneven distribution of light in a diffraction grating spectrum, *Phil. Magm*, Vol. 4, 1902, pp. 396-402.
[4]. U. Fano, The Theory of Anomalous Diffraction Gratings and of Quasi-stationary Waves on Metallic Surfaces (Sommerfeld's Waves), *J. Opt. Soc. Am*, Vol. 31, 1941, pp. 213-222.
[5]. T. Turbadar, Complete absorption of light by thin metal films, *Proc. Phys. Soc*, Vol. 73, 1959, pp. 40-44.
[6]. R. H. Ritchie, Plasma Losses by Fast Electrons in Thin Films, *Phys. Rev*, Vol. 106, 1957, pp. 874-881.
[7]. C. J. Powell and J. B. Swan, Origin of the Characteristic Electron Energy Losses in Aluminum, *Phys. Rev*, Vol. 115, 1959, pp. 869-875.
[8]. C. J. Powell and J. B. Swan, Effect of Oxidation on the Characteristic Loss Spectra of Aluminum and Magnesium, *Phys. Rev*, Vol. 118, 1960, pp. 640-643.
[9]. Y. Y Teng and E. A. Stern, Plasma Radiation from Metal Grating Surfaces, *Phys. Rev. Letters*, Vol. 19, 1967, pp. 511-514.
[10]. J. E. Stewart and W. S. Gallaway, Diffraction anomalies in. grating spectrometers, *Appl. Opt*, Vol. 1, 1962, pp. 421-429.
[11]. A. Hessel and A. A. Oliner, A new theory of Wood's anomalies on optical gratings, *Appl. Opt*, Vol. 10, 1965, pp. 1275-1299.
[12]. J. Hagglund and F. Sellberg, Reflection Absorption, and Emission of Light by Opaque Optical Gratings, *J. Opt. Soc. Am*, Vol. 56, 1966, pp. 1031-1040.
[13]. A. Otto, Excitation of Nonradiative Surface Plasma Waves in Silver by the Method of Frustrated Total Reflection, *Eitschrift f˙ur Physik*, Vol. 216, 1968, pp. 398-410.
[14]. E. Kretschmann and H. Raether, Radiative Decay of Non-radiative Surface Plasmons Excited by Light, *Z. Naturforsch*, Vol. 23, 1968, pp. 2135-2136.
[15]. E. Kretschmann, The Determination of the Optical Constants of Metals by Excitation of Surface Plasmons, *Z. Phys*, Vol. 241, 1971, pp. 313-324.
[16]. A. D. Boardman, Electromagnetic Surface Modes, *Wiley*, 1982.
[17]. V. M. Agranovitch and D. L. Mills, Surface Polaritons, *North-Holland*, 1982.
[18]. T. W. Ebbesen, H. J. Lezec, H. F. Ghaemi, T. Thio, and P. A. Wolff, Extraordinary optical transmission through subwavelength hole arrays, *Nature (London)*, Vol. 391, 1998, pp. 667-669.
[19]. H. F. Ghaemi, T. Thio, D. E. Grupp, T. W. Ebbesen, and H. J. Lezec, Surface plasmons enhance optical transmission through subwavelength holes, *Phys. Rev. B*, Vol. 58, 1998, pp. 6779-6782.
[20]. H. A. Bethe, Theory of diffraction by small holes, *Phys. Rev*, Vol. 66, 1944, pp. 163.
[21]. S. S. Jha, J. R. Kirtley, and J. C. Tsang, Intensity of Raman scattering from molecules adsorbed on a metallic grating, *Phys. Rev. B*, Vol. 22, 1980, pp. 3973-3982.
[22]. M. Moskovits, Surface-enhanced spectroscopy, *Rev. Mod. Phys*, Vol. 57, 1985, pp. 783-826.

[42]. H. X. Xu, E. J. Bjerneld, M. Kall, L. Borjesson, Spectroscopy of Single Hemoglobin Molecules by Surface Enhanced Raman Scattering, *Phys. Rev. Lett*, Vol. 83, 1999, pp. 4357-4360.

[24]. S. M. Nie, S. R. Emery, Probing single molecules and single nanoparticles by surface-enhanced Raman scattering, *Science*, Vol. 275, 1997, pp. 1102.

[25]. G. H. Agarwal and C. V. Kunasz, Dipole radiation in the presence of a rough surface. Conversion of a surface polariton field into radiation, *Phys. Rev. B*, Vol. 26, 1982, pp. 5832-5842.

[26]. P. T. Leung, Y. S. Kim, and T. F. George, Decay of molecules at corrugated thin metal films, *Phys. Rev. B*, Vol. 39, 1989, pp. 9888-9893.

[27]. R. K. Lee, O. J. Painter, B. D'Urso, A. Scherer, and A. Yariv, Measurement of spontaneous emission from a two dimensional photonic band gap defined microcavity at near-infrared wavelengths, *Appl. Phys. Lett*, Vol. 74, 1999, pp. 1522-1524.

[28]. H. Rigneault, F. Lemarchand, and A. Sentenac, Dipole radiation into grating structures, *J. Opt. Soc. Am. A*, Vol. 17, 2000, pp. 1048-1058.

[29]. K. W. Gossen and S. A. Lyon, Grating enhanced quantum well detector, *Appl. Phys. Lett*, Vol. 47, 1985, pp. 1257-1259.

[30]. D. Heitmann and U. Mackens, Grating-coupler-induced intersubband resonances in electron inversion layer of silicon, *Phys. Rev. B*, Vol. 33, 1986, pp. 8269-8283.

[31]. C. Gmachl, A. Straub, R. Colombelli, F. Capasso, D. L. Sivco, A. M. Sergent, and A. Y. Cho, Single-mode, tunable distributed feedback and multiple wavelength quantum cascade laser, *IEEE J. Quantum Electron*, Vol. 5, 2002, pp. 569-581.

[32]. A. Wittmann, M. Giovannini, J. Faist, L. Hvozdara, S. Blaser, D. Hofstetter, and E. Gini, Room temperature, continuous wave operation of distributed feedback quantum cascade lasers with widely spaced operation frequencies, *Appl. Phys. Lett*, Vol. 89, 2006, pp. 141116.

[33]. O. Demichel, L. Mahler, T. Losco, C. Mauro, R. Green, J. Xu, A. Trediccuci, F. Beltram, H. E. Beere, D. A. Richie, and V. Tamosiunas, Surface plasmon photonic structures in terahertz quantum cascade lasers, *Opt. Express*, Vol. 14, 2006, pp. 5335-5345.

[34]. S. Khanna, M. Lachab, A. G. Davies, E. H. Linfield, J. A. Fan, M. A. Belkin, and F. Capasso, Surface emitting terahertz quantum cascade laser with a double-metal waveguide, *Opt. Express*, Vol. 14, 2006, pp. 11672-11680.

[35]. R. W. Gruhlke, W. R. Holland, D. G. Hall, Surface plasmon cross coupling in molecular fluorescence near a corrugated thin metal film, *Phys. Rev. Lett*, Vol. 56, 1986, pp. 2838-2841.

[36]. D. K. Gifford and D. G. Hall, Emission through one of two metal electrodes of an organic light-emitting diode via surface-plasmon cross coupling, *Appl. Phys. Lett*, Vol. 81, 2002, pp. 4315-4317.

[37]. P. Andrew, W. L. Barnes, Energy transfer across a metal film mediated by surface plasmon polaritons, *Science*, Vol. 306, 2004, pp. 1002-1005.

[38]. J. R. Oppenheimer, Internal conversion in photosynthesis, *Phys. Rev*, Vol. 60, 1941, pp. 158-165.

[39]. M. M. Mekis, A. Dodabalapur, Laser action from two-dimensional distributed feedback in photonic crystals, *Appl. Phys. Lett*, Vol. 74, 1999, pp. 7-9.

[40]. C. Nylander, B. Liedberg, and T. Lind, Gas detection by means of surface plasmon resonance, *Sens. Actuators*, Vol. 3, 1982, pp. 79-88.

[41]. B. Liedberg, C. Nylander, and I. Lundström, Surface plasmons resonance for gas detection and biosensing, *Sens. Actuators*, Vol. 4, 1983, pp. 299-304.

[42]. GE Healthcare (http://www.biacore.com/lifesciences/index.html).

[43]. K. Nagata, H. Handa, Real-Time Analysis of Biomolecular Interactions: Applications of BIACORE, K. Nagata, H. Handa, *Springer Japan*, 1990.

[44]. N. F. Chiu, C. W. Lin, J. H. Lee, C. H. Kuan, K. C. Wu, and C. K. Lee, Enhanced luminescence of organic/metal nanostructure for grating coupler active longrange surface plasmonic device, *Appl. Phys. Lett*, Vol. 91, 2015, pp. 831141-831143.

[45]. N. F. Chiu, C. Yu, S. Y. Nien, J. H. Lee, C. H. Kuan, K. C. Wu, C. K. Lee and C. W. Lin, Enhancement and tunability of active plasmonic by multilayer grating coupled emission, *Opt. Express*, Vol. 15, 2007, pp. 11608-11615.

[46]. S. Y. Nien, N. F. Chiu, Y. H. Ho, J. H. Lee, C. W. Lin, K. C. Wu, C. K. Lee, J. R. Lin, M. K. Wei, and T. L. Chiu, Directional photoluminescence enhancement of organic emitters via surface plasmon coupling, *Appl. Phys. Lett* ,Vol. 94, 2009, pp. 1033041-1033043.

[47]. N. F. Chiu, S. Y. Nien, C. Yu, J. H. Lee and C. W. Lin, Advanced metal nanostructure design for surface plasmon photonic band-gap biosensor device, in *Proceedings of the 25th IEEE Conference on Medicine and Biology Society,* New York, USA, Aug 30-Sept 3, 2006*,* pp. 6521-6524.

[48]. J. Homola, S. S. Yee, G. Gauglitz, Surface Plasmon resonance sensor: review, *Sens. Actuators B*, Vol. 54, 1999, pp. 3-15.

[49]. J. Homola, I. Koudela, S. S. Yee, Surface Plasmon resonance sensor based on diffraction gratings and prism couplers: sensitivity comparison, *Sens. Actuators B*, Vol. 54, 1999, pp. 16-24.

[50]. S. H. Zaidi, M. Yousef and S. R. J. Brueck, Grating Coupling to Surface Plasma Waves. II. Interactions between First- and Second-Order Coupling, *J. of the Optical Society of America*, Vol. 8, 1991, pp. 1348-1359.

[51]. A. N. Grigorenko, P. I. Nikitin, and A. V. Kabashin, Phase jumps and interferometric surface plasmon resonance imaging, *Appl. Phys. Lett*, Vol. 75, 1999, pp. 3917-3919.

[52]. N. F. Chiu, C. D. Yang, Y. L. Kao and K. L. Lu, enhancing extraction of light from metal composite structures for plasmonic emitters using light-coupling effect, *Opt. Express,* Vol. 23, Issue 8, 2015, pp. 9602-9611.

[53]. N. F. Chiu, S. L. Lai, J. H. Lee, and C. W. Lin, Surface plasmon coupled emission in highly directional and sensitive plasmonic devices, *Proc. of SPIE*, Vol. 7192, 2009, pp. 71920I1-71920I8.

[54]. N. F. Chiu, C. H. Hou, C. J. Cheng and F. Y. Tsai, Plasmonic circular nanostructure for enhanced light absorption in organic solar cells, *Int J. Photoenergy,* Vol. 2013, 2013, pp. 1-7.

[55]. C.-W. Lin, N.-F. Chiu, J.-G. Huang, C.-K. Lee, Toward integrated Plasmonics for biosensing, in *Proceedings of the 5th International Conference on Nanochannels, Microchannels and Minichannels, (ASME ICNMM'07),* Puebla, Mexico, 18-20 June 2007, Invited Paper.

[56]. W. S. Hu, Z. G. Liu, J. Sun, S. N. Zhu, Q. Q. Xu, D. Feng, and Z. M. Ji, Optical properties of pulsed laser deposited ZnO thin films, *J. Phys. Chem. Solids*, Vol. 58, 1997, pp. 11441-11445.

[57]. S. C. Kitson, W. L. Barnes, and J. R. Samblesc, Surface Plasmon energy gaps and photoluminescence, *Phys. Rev. B*, Vol. 52, 1995, pp. 11441-11445.

[58]. N. F. Chiu, J. H. Lee, F. Y. Tsai, K. C. Liu, C. N. Lee, C. K. Lee and C. W. Lin, Light control in organic electroluminescence devices by plasmonic grating coupled emission for biochemical applications, *Phys. Proc. of SPIE*, Vol. 7192, 2009, pp. 71920I1-71920I8.

[59]. N. F. Chiu, C. J. Cheng, and T. Y. Huang, Organic plasmon-emitting for detecting refractive index variation, *Sensors*, Vol. 13, 2013, pp. 8340-8351.

[60]. N. F. Chiu, Y. C. Yen, Active Plasmonic Biosensors, *in Proceedings of the 1st International Conference on Advances in Sensors, Actuators, Metering and Sensing (ALLSENSORS'16),* Venice, Italy, April 24 – 28, 2016, pp. 32-34.
